International Journal of Renewable Energy Technology Research
Vol. 4, No. 3, May 2015, pp. 1- 20, ISSN: 2325 - 3924 (Online)
Available online at http://ijretr.org

Research article

THERMAL ENERGY NUMERICAL OPTIMIZATION OF BUILDING INTEGRATED SEMITRANSPARENT PHOTOVOLTAIC THERMAL SYSTEMS (BISPVT)

Ekoe a Akata Aloys Martial [(a)]*, Donatien Njomo [(a)], Basant Agrawal [(b)]

[(a)]Environmental Energy Technologies Laboratory (EETL), University of Yaoundé I, Cameroon
[(b)]Centre for Energy Studies, Indian Institute of Technology Delhi, Hauz Khas, New Delhi 110 016, India

E-mail : ekoealoys@yahoo.fr

ABSTRACT

Building integrated photovoltaic thermal system (BIPVT) has the potential to become one of the principal sources of renewable energy for domestic purpose. In this paper, a Building integrated semitransparent photovoltaic thermal system (BISPVT) system having fins at the back sheet of the photovoltaic module has been simulated. It has been observed that this system produces higher thermal and electrical efficiencies. The increase of wind velocity by fan system and heat exchange surface accelerates the convective heat transfer between the finned surface and the fluid flowing in the duct. The system area of 36.45 m^2 is capable of annually producing an amount of thermal energy of 76.66 kWh at an overall thermal efficiency of 56.07 %.

Keywords: Building Integrated Photovoltaic thermal (BIPVT), Passive design, Energy Conservation, Solar energy

*Corresponding author: ekoealoys@yahoo.fr (Ekoe a Akata Aloys Martial). Tel : 237 76317345 / 237 96326443

1. Introduction

The LRE building at EPFL in Lausanne – Switzerland, the NESTE Chemicals building in Helsinki – Finland, The Brundtland Centre atrium in Toftlund – Denmark, etc. show that solar energy systems can play an important role in reducing building energy consumption[1]. Building integrated photovoltaic (BIPV) has significant influence on the heat transfer through the building envelope because of the change of the thermal resistance by adding or replacing building elements such as roof tiles, facade elements, and shading devices with photovoltaic modules that perform the same function but also provides electrical power. Ciampi et al. [2] show that carefully designed ventilated facades, walls and roofs can considerably reduce the summer thermal loads.

The technological innovation in photovoltaic (PV) technology has been on the rise in the recent past years as a measure for cost reduction as well as broadening its application, where the PVs are integrated in the building or non-building structures for energy production and providing other functions of the structure. The most rapidly expanding market in the development of building integrated photovoltaic thermal (BIPVT) systems is seen in the developing countries for onsite power generation and space heating [3, 4]. The BIPVT is not widely use because its advantages compared to traditional PV modules and solar thermal collectors are unclear. Veronique et al. demonstrate that the BIPVT is more benefits than the simple integration [5]. Kimura [6], Taleb et al. [7], and Zhai et al. [8] have illustrated various methods of installing PV modules into a building for a concept of green building. Fig.1 shows a brief classification of BIPVT systems.

Dapeng Li et al. [9] investigates solar potential in urban residential buildings. They found that increasing building aspect ratio can raise building solar potential. Infield et al.[10] applied a steady state analysis model in a ventilated PV facade in order to evaluate an overall heat loss coefficient and thermal gain factor and suggested that the temperature of the PV module can be reduced by flowing air between the PV module and the double glass wall. Similar studies were carried out by Tripanagnostopoulos et al. [11], Zondag et al. [12], Prakash [13] and Chow [14] by flowing air and water below the PV module to increase the electrical efficiency of the PV module. The design of the thermal collector is according to the fluids flowing in the duct (air or water) [15]. Tiwari et al. [16] have evaluated the performance of the photovoltaic (PV) module integrated with air duct for composite climate of India. Analytical expression for overall energy efficiency (electrical and thermal) has been derived. It is observed that there is a fair agreement between theoretical and experimental observations and concluded that an overall energy efficiency of photovoltaic thermal (PVT) system is significantly increased by utilization of thermal energy in PV module. Similar results were found by Khaled et al. [17] and Parham et al. [18]. Maturi et al. [19] applicated an heat sink on the PV module back side to improve its performance. They recommend that passive strategy could be considered an effective solution to reduce the module working temperature and consequently to slightly increase its energy performance

Four numerical models have been built for the simulation of the thermal yield of a combined PV thermal collector by Zondag et al. [20]. They found that for the calculation of the daily yield, the simple 1D steady state model performs almost as good as the much more time-consuming 3D dynamical model. Fung et al.[21] presented a one-dimensional transient heat transfer model applicable to PV modules that have different orientations and inclinations, for evaluating the heat gain of semi-transparent photovoltaic modules for building integrated applications. Sarhaddi et al. [22] developed a thermal and electrical model to calculate the solar cell temperature, back surface temperature, outlet air temperature, open-circuit voltage, short-circuit current, maximum power point voltage, maximum power point current, etc. of a typical photovoltaic thermal (PVT) air collector and found that the results of numerical simulation are in good agreement with the experimental measurements. A modified equation for the exergy efficiency of a PVT air collector is derived in terms of design and climatic parameters [23]. João et al. compared the electric power generation of the photovoltaic panel with the solar radiation data. The photovoltaic system area of 16.5 m² was installed on the campus of UNIVATES University Center. They found that the solar potential of 4.11 kWh/m²/day is suitable for electricity generation from photovoltaic panels [24]. Peyvand et al. Use a wind-driven roof top turbine ventilator equipped

with a dynamo to cool down a photovoltaic (PV) cell. The experimental result of this combinaison show that is possible to reach an improvement of 46.54% in electricity production [25]. Agrawal et al. [26] optimized the opaque type BIPVT system for cold climatic conditions. The system fitted on the roof top of Srinagar over an effective area of 65 m^2 produces annually the electrical and thermal exergy of 16209 kWh and 1531 kWh. Agrawal et al. [27] also evaluated a hybrid micro-channel photovoltaic thermal (MCPVT) module. Such system has increased the overall thermal and exergy gains by 70.62% and 60.19% respectively. Vats et al. [28] evaluated a building integrated semitransparent photovoltaic thermal (BISPVT) system and found for an effective area of 5.44 m^2 that the overall annual thermal energy gain is 2497 kWh and electrical gain is 810 kWh. In this paper, analysis of the BISPVT is presented having fins at the back surface of PV modules.

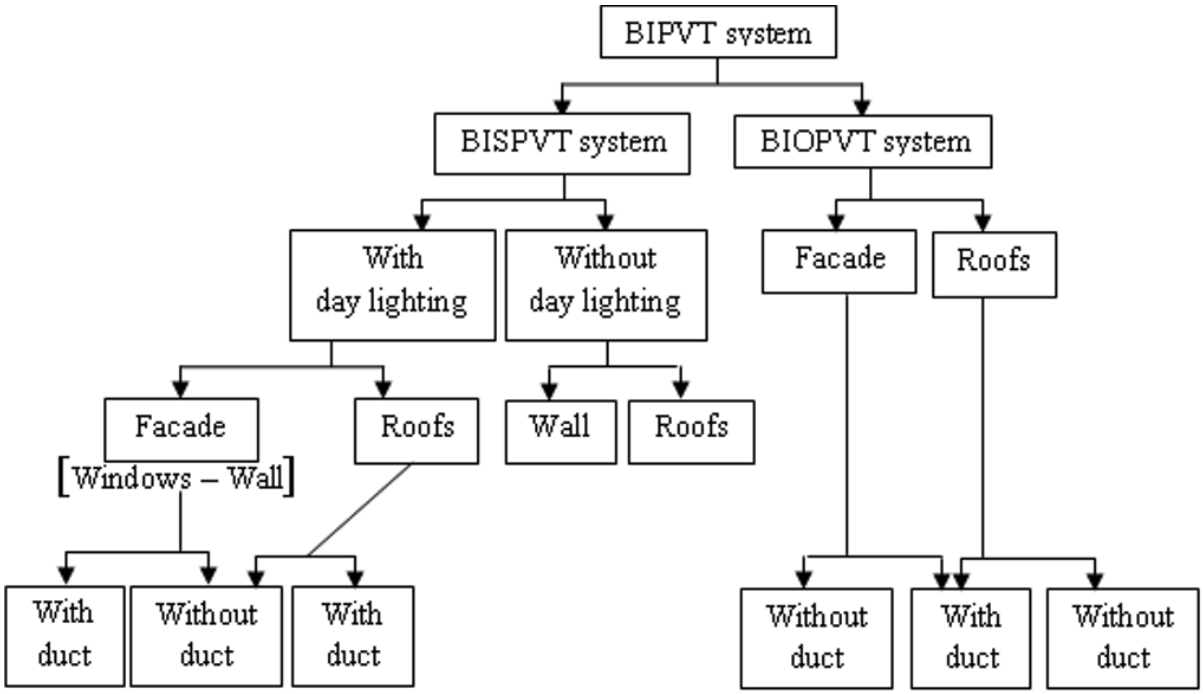

Fig. 1. Classification of BIPVT system

Parameters	Values
b	8.1 m
d	4.5 m
PV roof area	36,45 m^2
Roof inclination	12°
Volume of building	7152 m^3
C_f	0.38 [18]
Cair	1005 J $kg^{-1}K^{-1}$
α_C	0.9
α_T	0.5
β_C	0.83
τ_g	0.9
η_C	0.12 [17]

Table 1. Design parameters of a building and semitransparent PV module

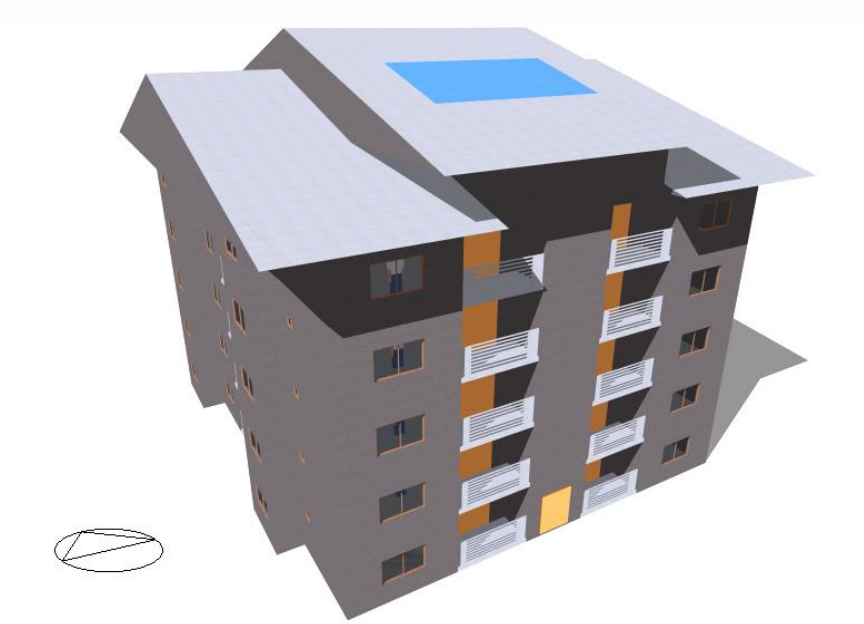

Fig. 2. (a). Building model

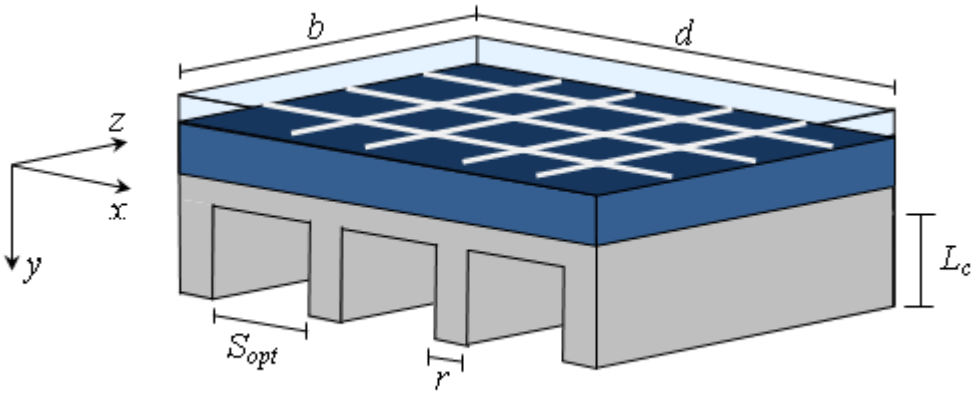

Fig. 2. (b). PV module of BISPVT system

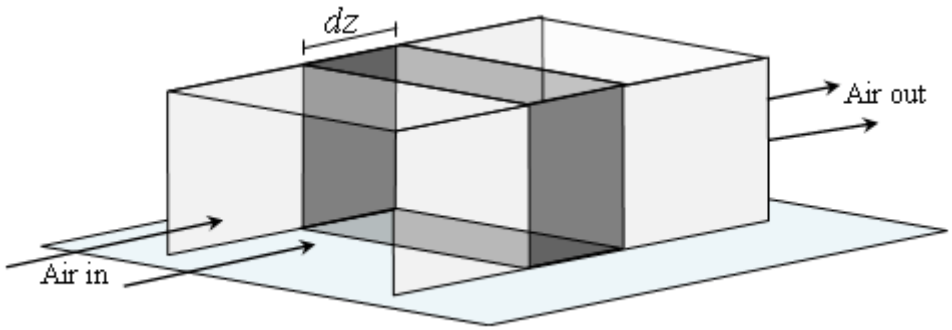

Fig. 3. Air flowing in the duct

2. Problem identification

Building lighting represent more than 15% of energy consumption in residential building, 25 - 35 % in office and commercial building in Cameroun. The electrical energy of BISPVT system of building under consideration is only used for the building light demand as 265W for each apartment (20 apartments) and 100W for corridor and outside light. The building under consideration is situated in Yaoundé at 3°52' N, 11°31' E. The size of the building is 26.65 m × 22.6 m with an average height of 15.3 m. The roof is south oriented and inclined at 12° to the horizontal. The building is insulated by a layer of sand and cement. Semitransparent photovoltaic thermal system is integrated as the roof top covering an effective area of 716.89 m^2. Fig. 2 shows the pictorial view of the BISPVT system. The BISPVT system is made of multicrystalline PV modules having rectangular fins. The depth of the duct is 8.1 m. The BISPVT system, area of 36.45 m^2, and made up of 30 PV modules and peak power of 5.4 kW is oriented in opposite direction with the wind to optimize the natural convection. The increases contact surface between the fluid flowing in the duct, by adding fins surfaces at the back sheet of PV module of BISPVT increase the heat exchange by convection, thereby decreasing the cells temperature while increasing the thermal energy extracted from the system.

3. Thermal modeling of BISPVT system

The following assumptions have been made to write the energy balance equation of BISPVT system

- One dimensional heat conduction is considered for the present study
- The system is in quasi-steady state

- There is no temperature stratification in the air of a room and semitransparent photovoltaic module
- Glass cover and the photovoltaic module are at a uniform temperature
- Air properties are constant with time and temperature

The energy balance for the different components of the building integrated semitransparent photovoltaic thermal system is as follows:

3.1. Solar cell of photovoltaic module.

Fig 2 shows an area $b.d$ of BISPVT system over which solar intensity is received. The energy balance for PV module of the building integrated semitransparent photovoltaic thermal system for an elemental area $b.dx$ is given by [26, 29, 30]:

$$\begin{bmatrix}\text{Rate of heat}\\ \text{received by}\\ \text{the solar cell}\end{bmatrix}=\begin{bmatrix}\text{Rate of heat loss from}\\ \text{PV module to ambient}\\ \text{air as the top loss}\end{bmatrix}+\begin{bmatrix}\text{Rate of heat loss}\\ \text{from PV module}\\ \text{to the back surface}\end{bmatrix}+\begin{bmatrix}\text{Rate of heat}\\ \text{received by the}\\ \text{non-packing area}\end{bmatrix}+\begin{bmatrix}\text{Rate of heat}\\ \text{generation}\end{bmatrix}$$

$$\tau_g\alpha_c\beta_c H(t)b.dx+\tau_g(1-\beta_c)\alpha_T H(t)b.dx=U_T(T_c-T_a)b.dx+h_{bs}(T_c-T_{bs})b.dx+\tau_g\alpha_c\beta_c\eta_c H(t)b.dx \quad (1)$$

After simplifying Eq. (1), the expression of a solar cell temperature can be obtained as

$$T_c=\frac{U_T T_a+h_{bs}T_{bs}+H(t)(\tau\alpha)_{eff}}{U_T+h_{bs}} \quad (2)$$

3.2. Back sheet of PV module

Following fig.2, energy balance for back surface of PV module is

$$\begin{bmatrix}\text{Rate of heat gain}\\ \text{from PV module}\\ \text{to the back surface}\end{bmatrix}=\begin{bmatrix}\text{Rate of heat loss}\\ \text{from the back surface}\\ \text{to air side in the duct}\end{bmatrix}+\begin{bmatrix}\text{Rate of heat}\\ \text{loss from the back}\\ \text{surface to fin surface}\end{bmatrix}$$

$$h_{bs}bd(T_c-T_{bs})=h_f b(d-n_{fin}r)(T_{bs}-T_f)-k_{bs}brn_{fin}\left.\frac{\partial T}{\partial y}\right|_{y=e_{bs}} \quad (3)$$

and

$$\frac{\partial^2 T}{\partial y^2}=0 \qquad 0\le y\le e_{bs}$$
$$T=T_c \qquad y=0$$
$$T=T_{bs} \qquad y=e_{bs} \quad (4)$$

After resolving Eq. (4), we obtained

$$\left.\frac{\partial T}{\partial y}\right|_{y=e_{bs}}=\frac{T_{bs}-T_c}{e_{bs}} \quad (5)$$

By substituting Eq. (5) in Eq. (3), the expression for the back surface temperature is obtained as

$$T_{bs}=\frac{h_{bs}(d-n_{fin}r)T_c+h_f(d-n_{fin}r)T_f}{(d-n_{fin}r)(h_{bs}+h_f)} \quad (6)$$

The convective coefficient between the back sheet of PV module and the air in the gap can be obtained as

$$h_f=\frac{Nu\,k_{bs}}{D_{du}} \quad (7)$$

where D_{du} is the hydraulic diameter

$$D_{du} = \frac{4A_{du}}{P_{du}} \tag{8}$$

Nu is the average Nusselt number for the thermal entrance region of flows between isothermal parallel plate of length L_c expressed as [31]

$$Nu = 7,54 + \frac{0,03(D_{du}/L_c)RePr}{1+0,016\left[(D_{du}/L_c)RePr\right]^{2/3}} \qquad forced\ convection \tag{9}$$

$$Nu = \frac{h_f S}{k_{bs}} = \left[\frac{576}{(Ra_S\, S/L_c)^2} + \frac{2,873}{(Ra_S\, S/L_c)^{0,5}}\right]^{-0,5} \qquad natural\ convecton \tag{10}$$

and the Rayleigh number Ra_S is expressed as

$$Ra_S = \frac{g\beta(\overline{T_b} - T_f)S^3}{\upsilon^2}\Pr \tag{11}$$

3.3. fin surface of Back sheet of PV module

Energy balance analysis on a differential volume element of the fin with the assumption of a one dimensional steady state reads

$$\begin{bmatrix} Net\ rate\ of\ heat\ gain\ by \\ conduction\ in\ y\ direction \\ into\ volume\ element\ \Delta y \end{bmatrix} + \begin{bmatrix} Net\ rate\ of\ heat\ gain\ by \\ convection\ through\ lateral \\ surfaces\ into\ volume\ element\ \Delta y \end{bmatrix} = 0$$

$$A_{bs}k_{bs}\frac{d^2T_b}{dy^2}.\Delta y + h_f(T_f - T_b)P.\Delta y = 0 \tag{12}$$

Δy is canceled and the result is rearranged to

$$m^2 = \frac{h_f P}{A_{bs}k_{bs}} \quad ; \quad \theta_b = T_b - T_f$$

$$\frac{d^2\theta_b}{dy^2} - m^2\theta_b = 0 \qquad 0 \le y \le L$$

$$\theta_b = T_{bs} - T_f \qquad y = 0 \tag{13}$$

$$k_{bs}\frac{d\theta_b}{dy} + h_f\theta_b = 0 \qquad y = L$$

Then, expression of fin surface temperature [32]is obtained as

$$\frac{T_b - T_f}{T_{bs} - T_f} = \frac{\cosh\left[m(L-y)\right] + \frac{h_f}{mk_{bs}}\sinh\left[m(L-y)\right]}{\cosh(mL) + \frac{h_f}{mk_{bs}}\sinh(mL)} \tag{14}$$

The fin tips, in practice, are exposed to the surroundings, and thus the proper boundary condition for the fin tip is of heat convection type that also includes the effects of radiation. The fin equation can still be solved in this

case using convection at the fin tip as the second boundary condition, but the analysis becomes more involved, and it results in rather lengthy expressions for the temperature distribution and the heat transfer. Yet, in general, the fin tip area is a small fraction of the total fin surface area, and thus the complexities involved can hardly justify the improvement in accuracy. A practical way of accounting for the heat loss from the fin tip is to replace the fin length L in the relation for the insulated tip case by a corrected length defined as [31]

$$L_c = L + \frac{A_c}{P} = L + \frac{r}{2} \tag{15}$$

Finally, the temperature expression of fin is given as

$$T_b(y) = \frac{\cosh\left[m(L_c - y)\right]}{\cosh(mL_c)}\left(T_{bs} - T_f\right) + T_f \tag{16}$$

A heat sink with closely packed fins will have greater surface area for heat transfer but a smaller heat transfer coefficient. A heat sink with widely spaced fins, on the other hand, will have a higher heat transfer coefficient but a smaller surface area. Therefore, there must be an optimum spacing S_{opt} that maximizes convection heat transfer from the heat sink for a given base area *b.d*, where *d* and *b* are the width and height of the base of the heat sink, respectively

$$S_{opt} = 2,714\left(\frac{S^3 d}{Ra_S}\right)^{0,25} = 2,714\frac{d}{Ra_d^{\,0,25}} \tag{17}$$

Where the Rayleigh number is expressed as

$$Ra_d = \frac{g\cos\theta\left(\overline{T_b} - T_f\right)\beta d^3}{\upsilon^2} Pr \tag{18}$$

$\overline{T_b}$ is the mean fin temperature given by

$$\overline{T_b} = \frac{1}{L_c}\int_0^{L_c} T_b(y)\,dy \;=\; T_f + \frac{T_{bs} - T_f}{mL_c}\frac{\sinh(mL_c)}{\cosh(mL_c)} \tag{19}$$

and the number of fin is given by

$$n_{fin} = \frac{d}{S_{opt} + r} \tag{20}$$

3.4. Air flowing in a duct

Following Fig.3 for each duct, energy balance for air flowing in the duct of the BISPVT system is given as

$$\begin{bmatrix} Rate\,of\ heat \\ received\ from\ the \\ back\ sheet\ to\ air \end{bmatrix} + \begin{bmatrix} Rate\,of\ heat \\ received\ from \\ fin\ surface\ to\ air \end{bmatrix} = \begin{bmatrix} Rate\,of\ heat\ gain \\ by\ air\ flowing \\ in\ the\ duct \end{bmatrix} + \begin{bmatrix} Rate\,of\ heat\ loss \\ from\ air\ through \\ insulation \end{bmatrix}$$

$$h_f\left(T_{bs} - T_f\right)S_{opt}dz + 2h_f\left(\overline{T_b} - T_f\right)L_c dz = \dot{m}_f c_f \frac{dT_f}{dz}dz + U_{ins}\left(T_f - T_r\right)S_{opt}dz \tag{21}$$

On integrating Eq. (21) with boundary condition $T_f(z=0) = T_{air,in}$ and $T_f(z=b) = T_{air,out}$ the flowing air temperature of BISPVT system for each duct of back sheet of PV module is given by

International Journal of Renewable Energy Technology Research
Vol. 4, No. 3, May 2015, pp. 1- 20, ISSN: 2325 - 3924 (Online)
Available online at http://ijretr.org

$$T_f(z)=\left(T_{air,in}-\frac{F_f}{G_f}\right)\exp\left(-G_f z\right)+\frac{F_f}{G_f} \tag{22}$$

Where

$$G_f=\frac{1}{\dot{m}_f c_f}\left[\left(h_f S_{opt}+\frac{2h_f}{m}\frac{\sinh(ml_c)}{\cosh(ml_c)}\right)\left(1-\frac{h_f\left(U_T+h_{bs}\right)}{\left(h_{bs}+h_f\right)\left(U_T+h_{bs}\right)-h_{bs}^2}\right)+U_{ins}S_{opt}\right]$$

$$F_f=\frac{U_{ins}S_{opt}}{\dot{m}_f c_f}T_r+\frac{1}{\dot{m}_f c_f}\left[h_f S_{opt}+\frac{2h_f}{m}\frac{\sinh(ml_c)}{\cosh(ml_c)}\right]\frac{h_{bs}\left[U_T T_a+H(t).(\tau\alpha)_{eff}\right]}{\left(h_{bs}+h_f\right)\left(U_T+h_{bs}\right)-h_{bs}^{\ 2}}$$

and the average air temperature of the air flowing in each duct of back sheet of PV module is given by

$$\overline{T_f}=\frac{1}{b}\int_0^b T_f(z)\,dz=\frac{F_f}{G_f}+\frac{1}{G_f b}\left(T_{air,in}-\frac{F_f}{G_f}\right)\left[1-\exp\left(-G_f b\right)\right] \tag{23}$$

The rate of useful thermal energy obtained for n_{PV} module of BISPVT system is given by

$$\dot{Q}_{useful,heat}=n_{PV}\left[n_{du}\dot{m}_f c_f\left(T_{air,out}-T_r\right)\right] \tag{24}$$

when air flowing in ducts is used to warm the ambient air inside the building
or given by

$$\dot{Q}_{useful,cool}=-n_{PV}\left[n_{du}\dot{m}_f c_f\left(T_{air,out}-T_{air,\,cool}\right)\right]$$

when air flowing in ducts is to be used in a cooling system

The outlet air temperature of the flowing air in each duct of the BISPVT system is

$$T_{air,out}=\left(T_{air,in}-\frac{F_f}{G_f}\right)\exp\left(-G_f b\right)+\frac{F_f}{G_f} \tag{25}$$

3.5. Building air temperature

The energy balance for the space heating of the building is given by

$$\begin{bmatrix}Rate\,of\ increase\\ of\ internal\ enrgy\end{bmatrix}=\begin{bmatrix}Rate\,of\ energy\\ generation\end{bmatrix}+\begin{bmatrix}Rate\,of\ heat\\ gain/loss\end{bmatrix}$$

$$\dot{m}_r c_{air}\frac{dT_r}{dt}=\dot{Q}_{useful,heat/cool}+(UA)_t\left(T_a-T_r\right)+U_{ins}A_{BISPVT}\left(\overline{T_f}-T_r\right)-0{,}33N_oV\left(T_a-T_r\right) \tag{26}$$

On solving Eq. (26) and applying the initial condition $T_r(t=0)=T_{ri}$, the building air temperature is obtained as

$$T_r=\left(T_{ri}-\frac{F_r}{G_r}\right)\exp\left(-G_r t\right)+\frac{F_r}{G_r} \tag{27}$$

Where

$$G_r = \frac{1}{m_r c_{air}} \left[\begin{array}{l} n_{pv} n_{du} \dot{m}_f c_f \left(1 - \frac{U_{ins} S_{opt}}{G_f \dot{m}_f c_f} \left(1 - e^{-G_f b} \right) \right) + (UA)_t - 0.33 N_0 V \\ + U_{ins} A_{bispvt} \left(1 - \frac{U_{ins} S_{opt}}{G_f \dot{m}_f c_f} \left(1 - \frac{1 - e^{-G_f b}}{G_f b} \right) \right) \end{array} \right]$$

$$F_r = \frac{1}{m_r c_{air}} \left[\begin{array}{l} n_{pv} n_{du} \dot{m}_f c_f \left(\begin{array}{l} \frac{1}{\dot{m}_f c_f G_f} \left[h_f S_{opt} + \frac{2h_f}{m} \frac{\sinh(ml_c)}{\cosh(ml_c)} \right] \frac{h_{bs} \left[U_T T_a + H(t).(\tau\alpha)_{eff} \right]}{(h_{bs} + h_f)(U_T + h_{bs}) - h_{bs}^2} \\ \times \left(1 - e^{-G_f b} \right) + T_{air,in} e^{-G_f b} \end{array} \right) \\ + \left((UA)_t - 0.33 N_0 V \right) T_a \\ + U_{ins} A_{bispvt} \left(\begin{array}{l} \frac{1}{\dot{m}_f c_f G_f} \left[h_f S_{opt} + \frac{2h_f}{m} \frac{\sinh(ml_c)}{\cosh(ml_c)} \right] \frac{h_{bs} \left[U_T T_a + H(t).(\tau\alpha)_{eff} \right]}{(h_{bs} + h_f)(U_T + h_{bs}) - h_{bs}^2} \\ \times \left(1 - \frac{1 - e^{-G_f b}}{G_f b} \right) + \frac{T_{air,in}}{G_f b} \left(1 - e^{-G_f b} \right) \end{array} \right) \end{array} \right]$$

3.6. Electrical energy, thermal energy and exergy of BISPVT system

3.6.1. Electrical energy of BISPVT system

According to [28], the hourly electrical efficiency of the PV module is given by

$$\eta_{PV,hourly} = \eta_{ref,PV} \left[1 - \beta_{ref,PV} \left(T_{c,hourly} - 25 \right) \right] \tag{28.a}$$

$$\eta_{TH,hourly} = \frac{\frac{\eta_{PV,hourly} H(t) n_{PV} A_{bispvt}}{C_f} + Q_{useful,hourly}}{H(t) n_{PV} A_{bispvt}} \tag{28.b}$$

where $\eta_{ref,PV}$ and $\beta_{ref,PV}$ are module efficiency and temperature coefficient for different PV materials.

The electrical power is

$$\begin{aligned} E_{el,hourly} &= \eta_{PV,hourly} A_{BISPVT} H(t)_{hourly} \\ E_{el,daily} &= \sum_{i=1}^{N_1} E_{el,hourly,i} \\ E_{el,monthly} &= n_o E_{el,daily} \\ E_{el,annual} &= \sum_{j=1}^{12} E_{el,monthly,j} \end{aligned} \tag{29}$$

where N_1 and n_o are the number of sunshine hours per day and the number of clear days in a month

3.6.2. Thermal energy of BISPVT system

The thermal energy is given by

$$Q_{th,daily} = \sum_{i=1}^{N_1} Q_{useful,hourly,i}$$
$$Q_{th,monthly} = \sum_{j=1}^{n_o} Q_{th,daily,j} \quad (30)$$
$$Q_{th,annual} = \sum_{k=1}^{12} Q_{th,monthly,k}$$

3.6.3. Exergy of BISPVT system

Exergy is defined as the maximum theoretical work obtainable from the interaction of a system with its environment until the equilibrium state between both is reached [28]. As there is a temperature difference between hot air coming out of the BIPVT system as a heat source and the atmospheric air as a heat sink, thermal energy can be transformed into work. The magnitude of transformable thermal energy to work is restricted by the Carnot efficiency. Thus, from the instantaneous quantity of heat produced by the BIPVT system, instantaneous thermal exergy [26],

$$Ex_{th,monthly} = Q_{th,monthly}\left(1-\frac{T_a}{T_{air,out}}\right) \quad (31)$$
$$Ex_{th,annual} = \sum_{i=1}^{12} Ex_{th,monthly,k}$$

and the overall exergy is the sum of annual exergy and the annual electrical energy

$$Ex_{annual} = Ex_{th,annual} + E_{el,annual} \quad (32)$$

4. Methodologies

In order to obtain the dynamic behavior of the system, as well as estimating the outlet air temperature from the duct of PV module for different season of the year, we used hourly global and diffuse solar radiation data of a representative day of each month (Klein day) over Yaoundé region for the 2011 year obtained from the Energy and Environmental Technologies Laboratory of the Department of Physics at the University of Yaoundé I; we also used climatic data issued by the Atmospheric Physics Laboratory.

1- The total solar radiation over inclined roof (21°) is obtained as [33]

$$H(t) = \left[H_g(t) - H_d(t)\right]R_b + \frac{1}{2}(1+\cos\theta)H_d(t) + \frac{1}{2}(1-\cos\theta)\rho_{alb}H_g(t) \quad (33)$$

2- The expression of cell temperature from Eq. (2) is introduced in Eq. (6) to have expression of back sheet of PV temperature as a function of fluid temperature.

3- The difference $\overline{T}_b - T_f$ is derived from Eq. (19)

These expressions are introduced in Eq. (21) and integrated to have the air flow temperature expression (Eq. (22)). Eq. (23) and Eq. (24) are used to solve Eq. (26).

4- The hourly thermal energy is obtained with the help of Eq. (24).

5- The hourly thermal energy from fin to air flowing in the duct is obtained with the help of Eq. (34)

$$Q_{fin-air} = n_{fins}(2L_c b)h_f\left(T_b - T_f\right) \quad (34)$$

6- The overall electrical and thermal efficiency are calculated by using Eq. (28).

7- Design specification and operating parameters of the building are presented in tables 1. These have been used as input parameters for energy analysis.

International Journal of Renewable Energy Technology Research
Vol. 4, No. 3, May 2015, pp. 1- 20, ISSN: 2325 - 3924 (Online)
Available online at http://ijretr.org

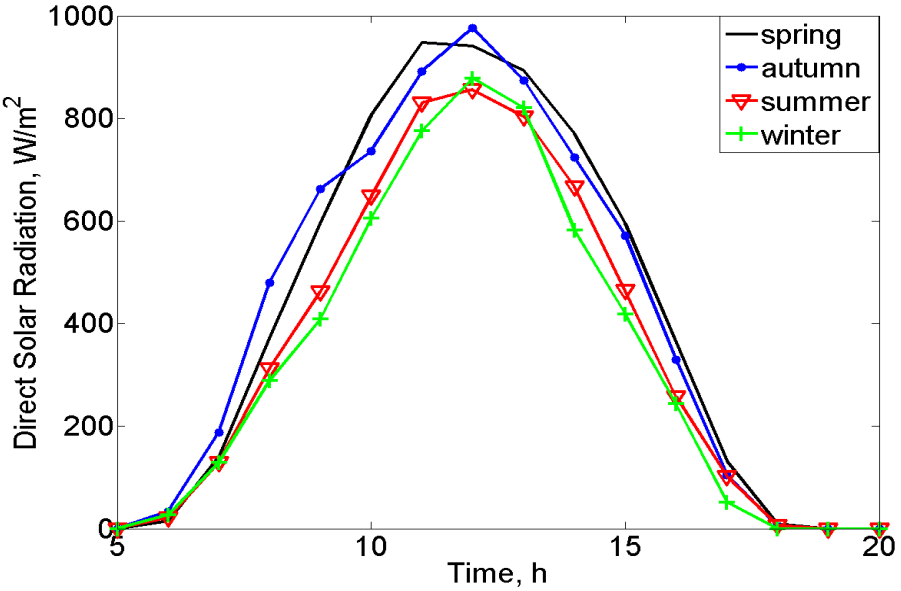

Fig. 4 Total solar radiation over inclined surface

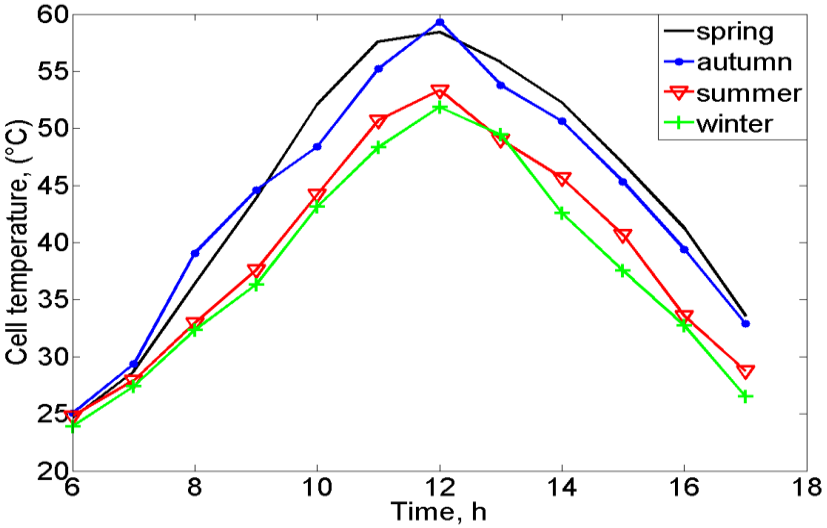

Fig. 5 (a). Cell temperature

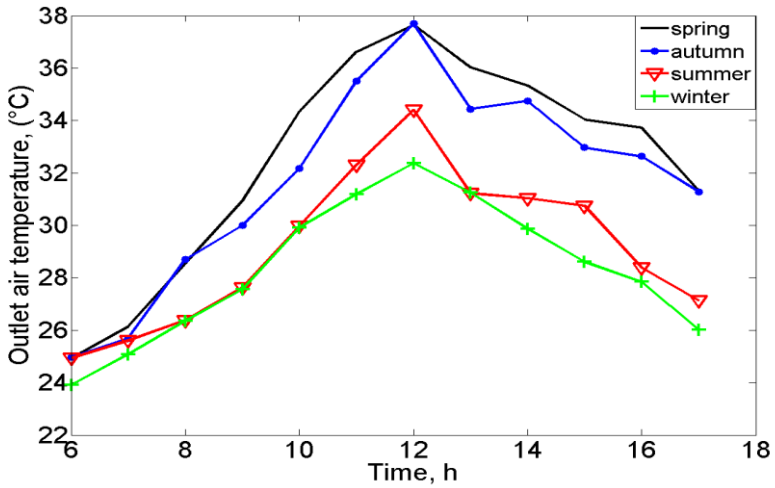

Fig. 5 (b). Outlet air temperature

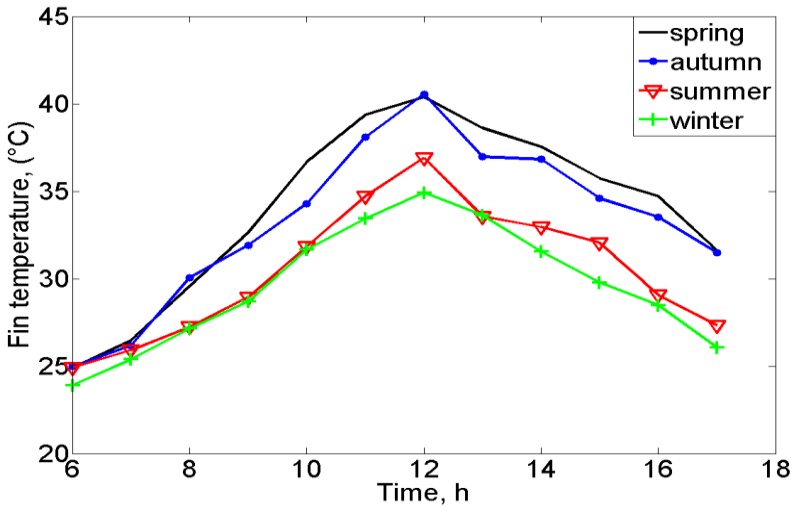

Fig. 5 (c). Fin temperature

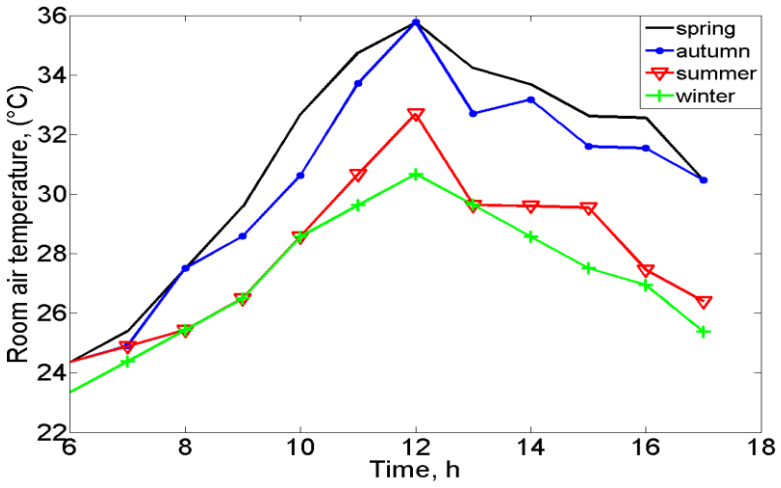

Fig. 5 (d). Room air temperature

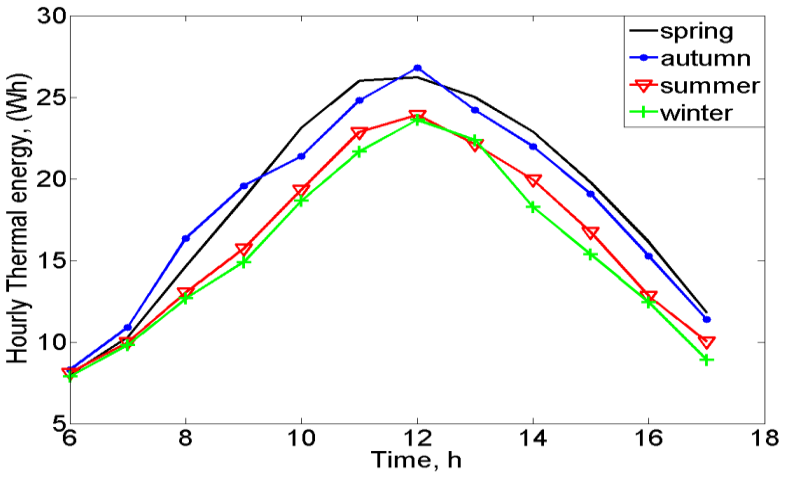

Fig. 6 Hourly thermal energy

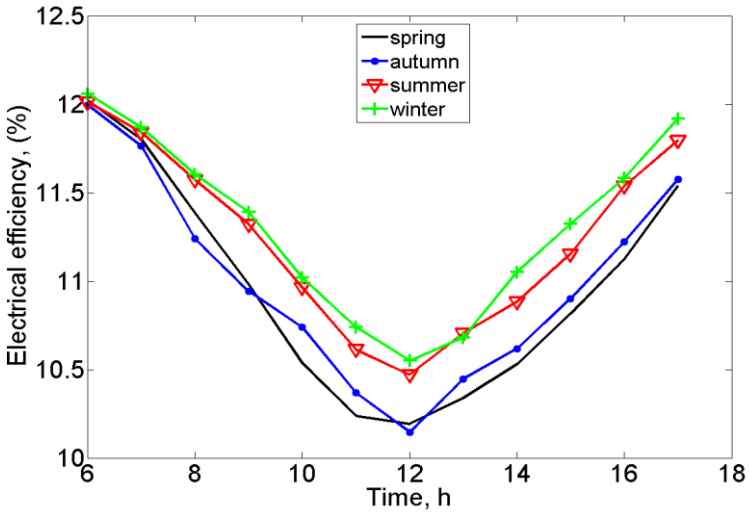

Fig. 7 (a). Hourly Electrical efficiency

International Journal of Renewable Energy Technology Research
Vol. 4, No. 3, May 2015, pp. 1- 20, ISSN: 2325 - 3924 (Online)
Available online at http://ijretr.org

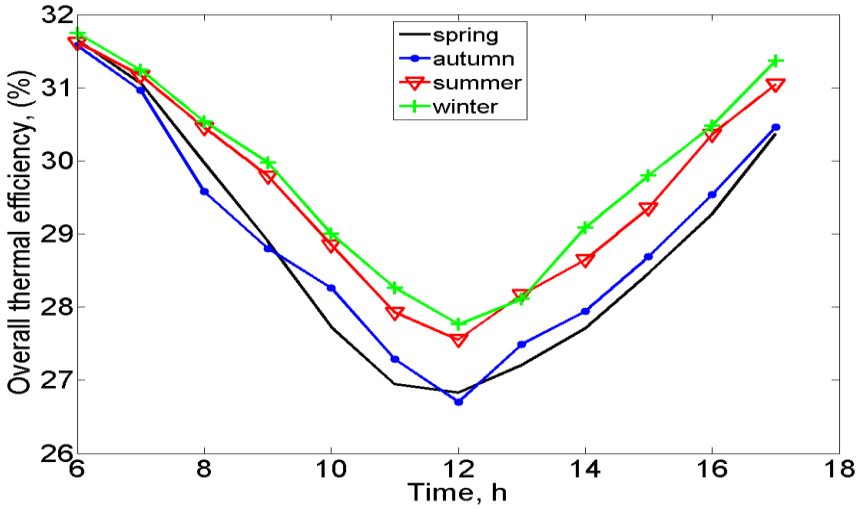

Fig. 7 (b). Hourly Thermal efficiency

5. Results and discussion

The variations of total solar intensity in Yaoundé for the four seasons of the year 2011 obtained from the Environmental Energy Technologies Laboratory (EETL) at the University of Yaoundé I are shown in Fig. 4. The values of various design parameters of the building and the semitransparent PV modules are given in Table.1. The hourly variation of cell temperature, outlet air temperature and fin temperature are shown in Fig. 5. From the figure, it is observe that the maximum temperature is 59.32 °C for cell temperature, 40.53 °C for fins surface and 37.69 °C for air flowing in the duct. The hourly thermal energy is shown in Fig. 6. Fig. 7 shows the hourly electrical and thermal efficiency of the BIPVT system. From, the above figures, it is observed that an increase in cell temperature decreases the cell efficiency.

The hourly variation of heat received from fins surfaces to air flowing in the duct is shown in Fig. 8. From the figure, it is observed that the maximum value of heat is 25.485 Wh. In a year heat extracted by air from fin surface is 55.4 kWh/an.

Fig. 9 shows the variation of the maximum value of cell temperature and electrical efficiency with the convection coefficient of fluid flowing in the duct for 12.00 a.m. It is observed that the maximum value of cell temperature decreased from 62.68 °C to 53.75 °C corresponding to an increase of the electrical efficiency of 0.75 % for a constant wind velocity of 0.9 ms^{-1}.

The variation of cell temperature and electrical efficiency with wind velocity of air flowing in the duct is shown in Fig. 10. It is observed that an increase of the wind velocity by a fan system from 0.1 ms^{-1} to 5 ms^{-1} decreases cell temperature from 66.92 °C to 43.3 °C corresponding to an increase of the electrical efficiency of 1.54 % at a constant convection coefficient of fluid flowing in the duct of 5 W/m^2K.

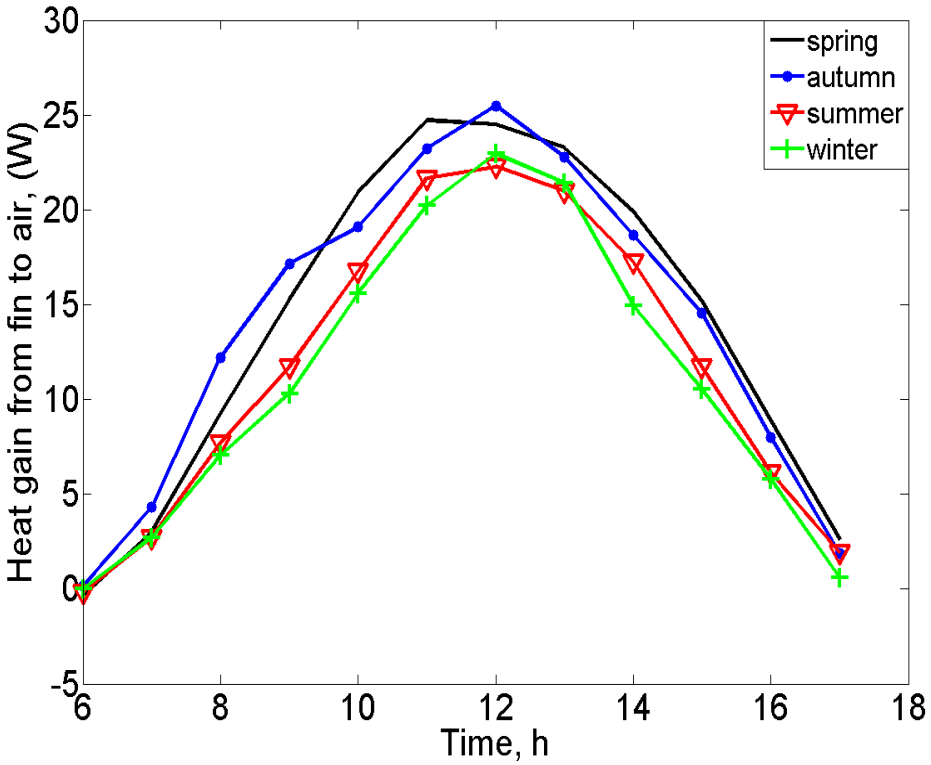

Fig. 8 Heat received from fin to air flowing

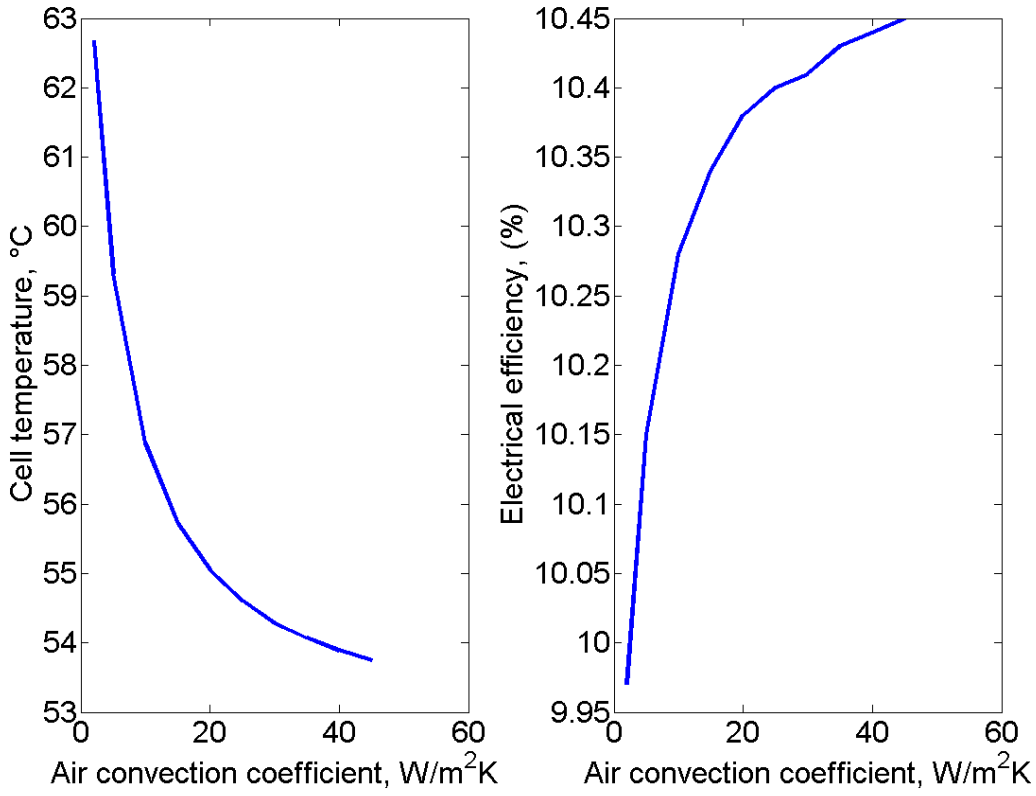

Fig. 9 Cell temperature and electrical efficiency with air convection coefficient

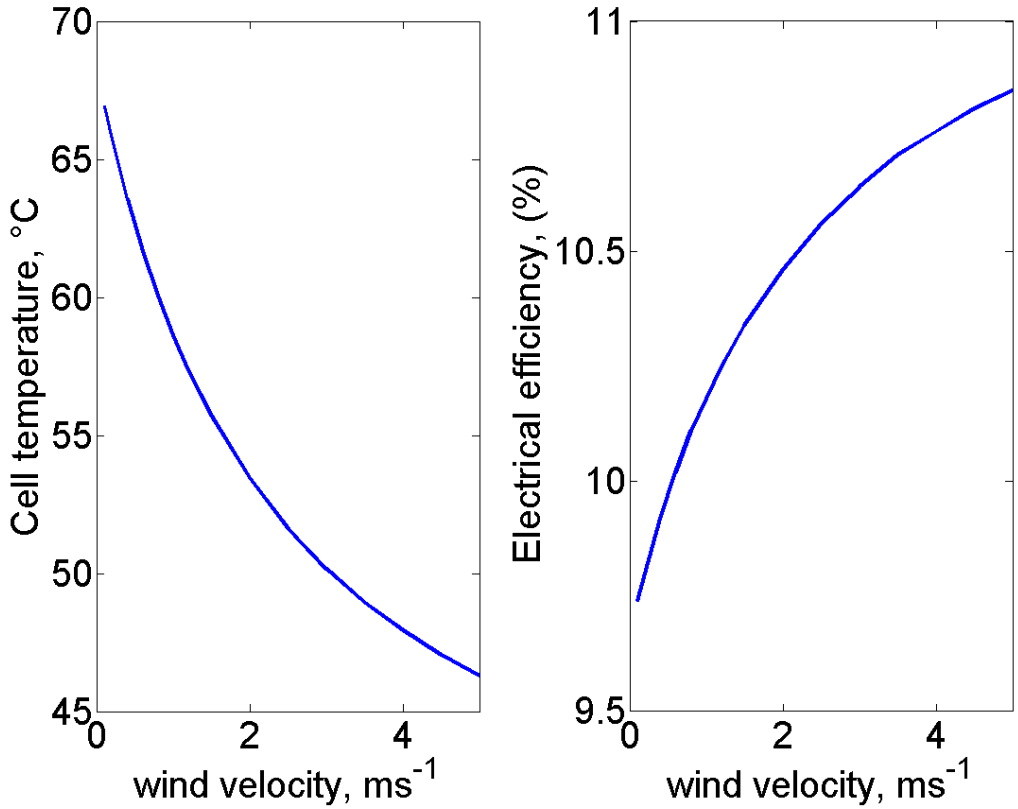

Fig. 10 Cell temperature and electrical efficiency with wind velocity

6. Conclusion

The thermal analysis of a building integrated semitransparent photovoltaic system with fins at the back surface of the PV module to increase the thermal energy of fluid flowing in the duct has been studied. It has been observed that:

- the decrease of cell temperature increases the electrical efficiency of PV module
- the maximum value of heat received from fins surfaces to air flowing in the duct is 25.485 Wh and heat extracted by air from the fin surface in a year is 55.4 kWh/year.
- an increase in the flow velocity of air flowing in the duct of BISPVT system from 0.1 to 5 ms^{-1} by a fan system can decreases the cell temperature from 66.92 °C to 43.3 °C corresponding to an increase of the electrical efficiency of 1.54 %

The BISPVT system studied produces a maximum annual thermal energy of 76.66 kWh with an overall thermal efficiency of 56.07 %.

Appendix A

$$(\tau\alpha)_{eff} = \tau_g\left[\alpha_c\beta_c + \alpha_T(1-\beta_c) - \alpha_c\beta_c\eta_c\right]$$

$$U_T = \left(\frac{e_g}{k_g} + \frac{1}{h_0}\right)^{-1}$$

$$U_{ins} = \left(\frac{e_{Al}}{k_{Al}} + \frac{1}{h_0} + \frac{e_{cpl}}{k_{cpl}} \right)^{-1}$$

$$h_0 = 5.7 + 3.8\,v$$

$$h_{bs} = \left(\frac{e_{bs}}{k_{bs}} \right)^{-1}$$

Nomenclature

A	area (m^2)
b	height of the BISPVT system (m)
c	specific heat (J/kg K)
d	width of the BISPVT system (m)
dx	elemental length (m)
dy	elemental length (m)
dz	elemental length (m)
dt	elemental time (s)
D	hydraulic diameter (m)
e	thickness (m)
g	thermal gain factor
h	heat transfer coefficient (W/m^2K)
k	thermal conductivity (W/mK)
L	length (m)
Lc	corrected length (m)
$\dot{m}$	Mass flow rate (kg/s)
n	number
Nu	Nusselt number (dimensionless)
Pr	Prandtl number (dimensionless)
r	fin's thickness (m)
Ra	Rayleigh number (dimensionless)
Re	Reynolds number (dimensionless)
S	distance between two fins (m)
T	temperature (K)
$H(t)$	Incident solar radiation (W/m^2)
U	overall heat transfer coefficient (W/m^2K)
$(UA)_t$	overall heat transfer coefficient from room to ambient air (W/K)
V	volume (m^3), velocity (m/s)

Greek symbols

α	absorptivity
β	packing factor, volume expansion Coefficient
θ	inclination of roof (rad)
τ	transmissivity
η	efficiency
$(\alpha\tau)_{eff}$	product of effective absorptivity and transmittivity
ρ_{alb}	albedo

References

[1] Hestnes AG. Building Integration of Solar Energy Systems, Solar Energy 67 (1999) 181-187.

[2] Ciampi M, Leccese F, Tuoni G, Ventilated facades energy performance in summer cooling of buildings, Solar Energy 75 (2003) 491-502.

[3] Tonui JK. Tripanagnostopoulos Y, Performance improvement of PV/T solar collectors with natural air flow operation, Solar Energy 82 (2008) 1-12.

[4] Bazilian MD, Prasad D, Modelling of a photovoltaic heat recovery system and its role in a design decision support tool for building professionals, Renewable Energy 27 (2002) 57-68.

[5] Véronique Delisle, Michaël Kummer. A novel approach to compare building integrated photovoltaics/thermal air collectors to side-by-side PV modules and solar thermal collectors. Solar Energy 100 (2014) 50–65

[6] Kimura K-i, Photovoltaic systems and architecture, Solar Energy Materials and Solar Cells 35 (1994) 409-419.

[7] Taleb HM, Pitts AC, The potential to exploit use of building-integrated photovoltaics in countries of the Gulf Cooperation Council, Renewable Energy 34 (2009) 1092-1099.

[8] Zhai XQ, Wang RZ, Dai YJ, Wu JY, Ma Q. Experience on integration of solar thermal technologies with green buildings. Renewable Energy. 2008;33:1904-10.

[9] Dapeng Li, Gang Liu, Shengming Liao. Solar potential in urban residential buildings. Solar Energy 111 (2015) 225–235

[10] Infield D, Mei L, Eicker U. Thermal performance estimation for ventilated PV facades, Solar Energy, 76 (2004) 93-98.

[11] Tripanagnostopoulos Y, Nousia T, Souliotis M, Yianoulis P, Hybrid photovoltaic/thermal solar systems, Solar Energy 72 (2002) 217-234.

[12] Zondag HA, de Vries DW, van Helden WGJ, van Zolingen RJC, van Steenhoven AA, The thermal and electrical yield of a PV-thermal collector, Solar Energy 72 (2002) 113-128.

[13] Prakash J. Transient analysis of a photovoltaic-thermal solar collector for co- generation of electricity and hot air/water, Energy Conversion and Management. 35 (1994) 967-972.

[14] Chow TT, Hand JW, Strachan PA, Building-integrated photovoltaic and thermal applications in a subtropical hotel building, Applied Thermal Engineering 23 (2003) 2035-2049.

[15] R. R. Avezov, J. S. Akhatov, and N. R. Avezova. A Review on Photovoltaic_Thermal (PV–T) Air and Water Collectors. Applied Solar Energy, 2011, Vol. 47, No. 3, pp. 169–183

[16] Tiwari A, Sodha MS, Chandra A, Joshi JC, Performance evaluation of photovoltaic thermal solar air collector for composite climate of India, Solar Energy Materials and Solar Cells 90(2006) 175-189.

[17] Khaled Touafeka, Mourad Haddadib, Ali Malek. Design and modeling of a photovoltaic thermal collector for domestic air heating and electricity production. Energy and Buildings 59 (2013) 21–28

[18] Parham A. Mirzaei, Enrico Paterna, Jan Carmeliet. Investigation of the role of cavity airflow on the performance of building-integrated photovoltaic panels. Solar Energy 107 (2014) 510–522

[19] Laura Maturi, Roberto Lollini, David Moser, Wolfram Sparber. Experimental investigation of a low cost passive strategy to improve the performance of Building Integrated Photovoltaic systems. Solar Energy 111 (2015) 288–296

[20] Zondag HA, de Vries DW, van Helden WGJ, van Zolingen RJC, van Steenhoven AA. The thermal and electrical yield of a PV–thermal collector. Sol Energy 2002; 72 (2): 113–28.

[21] Fung TYY, Yang H. Study on thermal performance of semi-transparent building- integrated photovoltaic glazings, Energy and Buildings 40 (2008) 341-350.

[22] Sarhaddi F, Farahat S, Ajam H, Behzadmehr A, Mahdavi Adeli M, An improved thermal and electrical model for a solar photovoltaic thermal (PV/T) air collector, Applied Energy 87 (2010) 2328-2339.

[23] Sarhaddi F, Farahat S, Ajam H, Behzadmehr A, Exergetic optimization of a solar photovoltaic thermal (PV/T) air collector, International Journal of Energy Research 35 (2011) 813-827.

[24] João Vicente Akwa, Odorico Konrad, Gustavo Vinícius Kaufmann, Cezar Augusto Machado. Evaluation of the Photovoltaic Generation Potential and Real-Time Analysis of the Photovoltaic Panel Operation on a Building Facade in Southern Brazil. Energy and building Accepted Manuscript PII: S0378-7788(13)00689-0; DOI: http://dx.doi.org/doi:10.1016/j.enbuild.2013.11.007 ; Reference: ENB 4608

[25] Peyvand Valeh-e-Sheyda, Masoud Rahimi1, Amin Parsamoghadam, Mohammad Moein Masahi. Using a wind-driven ventilator to enhance a photovoltaic cell power generation. Energy and building Accepted Manuscript (PII: S0378-7788(13)00869-4, DOI: http://dx.doi.org/doi:10.1016/j.enbuild.2013.12.052, Reference: ENB 4744)

[26] Agrawal B, Tiwari GN. Optimizing the energy and exergy of building integrated photovoltaic thermal (BIPVT) systems under cold climatic conditions, Applied Energy 87 (2010) 417-426.

[27] Agrawal B, Tiwari GN, Energy and exergy analysis of hybrid micro-channel photovoltaic thermal module, Solar Energy 85 (2011) 356-370.

[28] Vats K, Tiwari GN, Energy and exergy analysis of a building integrated semitransparent photovoltaic thermal (BISPVT) system, Applied Energy 96 (2012) 409-416.

[29] Vats K, Tiwari GN, Performance evaluation of a building integrated semitransparent photovoltaic thermal system for roof and façade, Energy and Buildings 45 (2012) 211-218.

[30] Dubey S, Sandhu GS, Tiwari GN, Analytical expression for electrical efficiency of PV/T hybrid air collector, Applied Energy 86 (2009) 697-705.

[31] Çengel YA, Heat Transfer: A Practical Approach: McGraw-Hill (2003).

[32] Özışık N, Heat transfer: a basic approach: McGraw-Hill (1985).

[33] Duffie JA, Beckman WA, Solar Engineering of Thermal Processes: Wiley (2013).